Adaptive Fast Terminal Sliding Mode Control of A Suspended Cable–Driven Robot

Mohammad isaac hosseini
Advanced Robotics and Automated Systems (ARAS)
K. N. Toosi University of Technology Tehran, lran.
mohammadisaac.hosseini@email.kntu.ac.ir

Mohammadreza Jafari harandi
Advanced Robotics and Automated Systems (ARAS)
K. N. Toosi University of Technology
Tehran, lran.
jafari@email.kntu.ac.ir

seyed ahmad khalilpour seyedi
Advanced Robotics and Automated Systems
K. N. Toosi University of Technology
Tehran, lran.
khalilpour@ee.kntu.ac.ir

Hamid reza Dokht taghirad
Advanced Robotics and Automated Systems (ARAS)
K. N. Toosi University of Technology
Tehran, lran.
taghirad@kntu.ac.ir

***Abstract*—Increasing the speed and precision of operation in cable robots is crucial due to the flexibility of cables. On the other hand, due to the frequent dynamical uncertainties present in cable robots, providing a robust control method is necessary. The performance of the fast terminal sliding mode (FTSM) controller has been investigated in various systems, which ensures that the state of the system is rapidly converged to the equilibrium point at a finite time. In this paper, the FTSM controller has been developed in such a way to be able to track the optimal robot path in the presence of dynamic uncertainties at different operating speeds. The main innovation of this paper is to provide an adaptive robust control method for controlling cable robots and analyzing the stability of the closed-loop control system based on the Lyapunov stability theory. In order to demonstrate the effectiveness of the proposed controller, simulation results, as well as experimental implementation on ARAS–CAM, a four cable suspended robot with three degrees of freedom, has been investigated and it is shown that the proposed controller can provide suitable tracking performance in practice.**

***Index Terms*—suspended cable-driven parallel manipulator, fast terminal sliding mode, finite-time convergence, robust control, adaptive control**

I. Introduction

In a cable–driven parallel manipulator (CDPM) the end effector is driven by several actuated cables that are connected to the base frame. Compared to other kinds of parallel robots, which use rigid body links, CDPMs have numerous advantages [1]. Large workspace, low stiffness, high accelerations, high payload to weight ratio and fast employability alongside with simple structure are just some of the features of these robots. Usage of CDPMs in practical applications such as material handling [2], instrumentation [3], rescue missions in dangerous environments [4], medical rehabilitation equipment [5], positioning devices [6] has been growing.

The requirement of unilateral tension in cables of CDPMs divides these kinds of robots into two groups: fully constrained and suspended. Fully constrained cable robots are designed using redundancy of actuators. In other words, actuators outnumber the degrees of freedom (DOF) of the system by at least one [7]. Also, extra cables could be used to enlarge workspace or optimize performance. In order to keep all the cables under tension in suspended mechanisms, a passive force such as gravity is used. These kinds of robots are known as cable–suspended parallel manipulators (CSPM) [8]. Even though researchers have developed various control techniques such as iterative learning control [9], optimal control [10], adaptive control [11], robust control [12] to control CDPMs, development of a control system for this group of robots is extremely complicated due to the characteristics of cables, and kinematic and dynamic uncertainties. These challenges inhibits finding an exact model for the system and limits the trajectory tracking of the controller. Sliding mode controller (SMC) is an effective control method that is used in linear and nonlinear systems such as robotic manipulators [13], electrical motors [14] and power systems [15] due to its simplicity, robustness, reduced order and simple implementation [16]. However, in this method system state approaches the equilibrium point

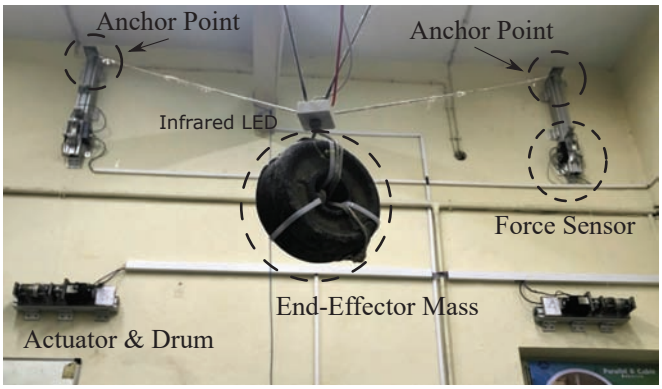

Fig. 1. ARAS-CAM cable-driven parallel robot

978-1-7281-1508-5/19/$31.00

just in an infinite time. As a solution, terminal sliding mode (TSM) controller has been developed in the literature. By using a fractional power term in the sliding surface [17], this controller guarantees the convergence of the system state to the equilibrium point in a finite time. The proposed solution entails a new problem that being far away from the origin, the system converges very slowly to the origin, even slower than SMC [18]. To solve this problem, fast terminal sliding mode (FTSM) controller was offered by Yu and Man [19]. In this method when the system state is far away from the equilibrium point, the controller approximates SMC dynamics. On the other hand, by becoming close to the equilibrium point, the controller behaves like a TSM controller.

The main contribution of this paper is develop an adaptive fast terminal sliding mode (A-FTSM) controller for the cable robot in order to obtain suitable the tracking performance in the presence of dynamic uncertainties. Furthermore to ensure closed-loop stability sufficient condition for the stability of the closed-loop system is derived based on the Lyapunov stability theorem. The proposed controller is implemented on ARAS–CAM, a four cable suspended robot with three degrees of freedom, illustrated in Fig1.

The remaining of the paper is organized as follows: Section II describes the kinematic and the dynamic modeling of ARAS-CAM. Section III is dedicated to the proposition and design of the proposed adaptive fast terminal sliding mode control scheme for the cable-driven robot. The real-time experimental validations of the proposed control scheme are presented in Section IV. Section V concludes this paper.

II. Kinematics and Dynamics of ARAS–CAM

A. Kinematics

In this section, kinematics, Jacobian and Dynamic equation of the robot which is shown in Fig.2 are given. The loop closure equation for this robot is given as follows

$$\mathbf{X} = \mathbf{X}_{A_i} + l_i \hat{\mathbf{s}}_\mathbf{i} \qquad \text{for } i = 1, \ldots, 4 \tag{1}$$

in which $\mathbf{X}$ is position vector of end-effector (moving platform) and $\mathbf{X}_{A_i}, l_i$ and $\hat{\mathbf{s}}_\mathbf{i}$ are position of i'th anchor point, cable length and direction vector of the cable, respectively. Using Eq.1, inverse kinematic is derived as:

$$l_i^2 = (\mathbf{X} - \mathbf{X}_{A_i})^T (\mathbf{X} - \mathbf{X}_{A_i}) \tag{2}$$

To derive Jacobian matrix, differentiate Eq.1 respect to time as follows

$$\dot{\mathbf{X}} = \dot{l}_i \hat{\mathbf{s}}_\mathbf{i} + l_i \dot{\hat{\mathbf{s}}}_\mathbf{i} \tag{3}$$

By dot multiple both sides of Eq.3 to $\hat{\mathbf{s}}_\mathbf{i}$, $\dot{l}_i$ is equal to

$$\dot{\mathbf{X}} \cdot \hat{\mathbf{s}}_\mathbf{i} = \dot{l}_i \hat{\mathbf{s}}_\mathbf{i}.\hat{\mathbf{s}}_\mathbf{i} + l_i \dot{\hat{\mathbf{s}}}_\mathbf{i}.\hat{\mathbf{s}}_\mathbf{i} \tag{4}$$

we know that $\dot{\hat{\mathbf{s}}}_\mathbf{i} \cdot \hat{\mathbf{s}}_\mathbf{i}$ is zero because $\dot{\hat{\mathbf{s}}}_\mathbf{i} = \dot{\alpha}(\hat{k} \times \hat{\mathbf{s}}_\mathbf{i})$ in which $\hat{k} = [0, 0, 1]^T$: is perpendicular to $\hat{\mathbf{s}}_\mathbf{i}$. Therefore, velocity loop closure of the robot is $\dot{l}_i = \hat{\mathbf{s}}_\mathbf{i}.\dot{\mathbf{X}}$ and Jacobian matrix is as follows

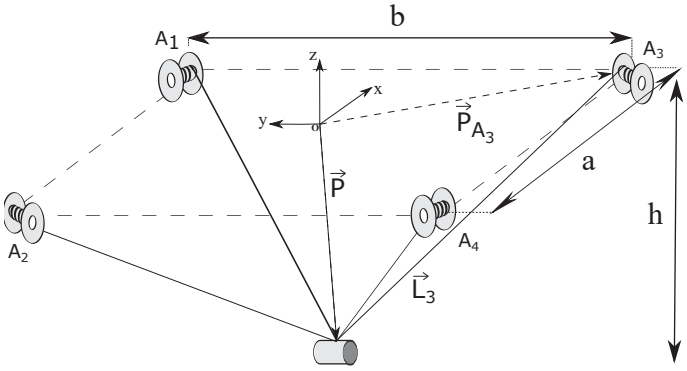

Fig. 2. The schematics of ARAS-CAM cable-driven robot

$$\dot{\mathbf{L}} = \mathbf{J}(\mathbf{X})\dot{\mathbf{X}} \qquad \mathbf{L} = \begin{bmatrix} l_1 \\ l_2 \\ l_3 \\ l_4 \end{bmatrix} \qquad \mathbf{X} = \begin{bmatrix} x \\ y \\ z \end{bmatrix}$$

$$\mathbf{J}(\mathbf{X}) = \begin{bmatrix} \frac{(x-x_{A_1})}{l_1} & \frac{(y-y_{A_1})}{l_1} & \frac{(z-z_{A_1})}{l_1} \\ \frac{(x-x_{A_2})}{l_2} & \frac{(y-y_{A_2})}{l_2} & \frac{(z-z_{A_2})}{l_2} \\ \frac{(x-x_{A_3})}{l_3} & \frac{(y-y_{A_3})}{l_3} & \frac{(z-z_{A_3})}{l_3} \\ \frac{(x-x_{A_4})}{l_4} & \frac{(y-y_{A_4})}{l_4} & \frac{(z-z_{A_4})}{l_4} \end{bmatrix} \tag{5}$$

B. Dynamics

Let us derive dynamic equations of the robot. Since the mass of end-effector is dominant compared to the mass of cables, we might neglect them. Thus with Newton-Euler equation for a mass with four acting forces on it, dynamic equations is derived as follows

$$\mathbf{M}(\mathbf{X})\ddot{\mathbf{X}} + \mathbf{C}(\mathbf{X}, \dot{\mathbf{X}})\dot{\mathbf{X}} + \mathbf{G}(\mathbf{X}) = -\mathbf{J}(\mathbf{X})^T \boldsymbol{\tau}$$

$$\mathbf{M}(\mathbf{X}) = \begin{bmatrix} m & 0 & 0 \\ 0 & m & 0 \\ 0 & 0 & m \end{bmatrix} \quad \mathbf{C}(\mathbf{X}, \dot{\mathbf{X}}) = 0 \quad \mathbf{G}(\mathbf{X}) = \begin{bmatrix} 0 \\ 0 \\ mg \end{bmatrix} \tag{6}$$

Some important properties of the dynamics equations are as follows [20].

P1: The inertia matrix $\mathbf{M}(\mathbf{X})$ is symmetric and positive definite for all $\mathbf{X}$.

P2: The matrix $\dot{\mathbf{M}}(\mathbf{X}) - 2\mathbf{C}(\mathbf{X}, \dot{\mathbf{X}})$ is skew symmetric.

P3: The dynamic model is linear with respect to a set of dynamical parameters and can be represented in a linear regression form:

$$\mathbf{M}(\mathbf{X})\ddot{\mathbf{X}} + \mathbf{C}(\mathbf{X}, \dot{\mathbf{X}})\dot{\mathbf{X}} + \mathbf{G}(\mathbf{X}) = \mathbf{Y}_m(\ddot{\mathbf{X}}, \dot{\mathbf{X}}, \mathbf{X})\boldsymbol{\theta}_m, \tag{7}$$

where $\mathbf{Y}_m(\ddot{\mathbf{X}}, \dot{\mathbf{X}}, \mathbf{X})$ denotes the regressor matrix and θ_m denotes the vector of dynamic parameters.

III. Adaptive FTSM Control Design

In this section an adaptive FTSM controller for 3-DOF suspended cable driven robot with uncertain dynamics is designed. In the proposed controller, trajectory tracking is guaranteed

by combination of finite time sliding mode controller and adaptation law for dynamic parameters. Before this, the concept of terminal sliding mode and fast terminal sliding mode is given.

Lemma 1. *[21]: Suppose that a positive function $\gamma(t)$ satisfies the following inequality*

$$\dot{\gamma}(t) \leq -\mu\gamma^{\eta}(t) \quad \forall t \geq t_0 \tag{8}$$

where μ is a positive constant and $\eta = \frac{p}{q}$ in which p, q are positive constants and $p < q$. Then $\gamma(t)$ satisfies the following inequality

$$\gamma^{1-\eta}(t) \leq \gamma^{1-\eta}(t_0) - \mu(1-\eta)(t-t_0) \quad t \geq t_0 \tag{9}$$

and the upper bound of time for $\gamma(t)$ to converges to zero is as follows

$$t_0 + \frac{\gamma^{1-\eta}(t_0)}{\mu(1-\eta)} \tag{10}$$

Lemma 2. *[19]: The solution of differential inequality 8 reach to zero in finite time, but if initial condition is large, the convergence rate is slow at the beginning. In order to overcome this problem, the term $-\alpha\gamma^{\beta}(t)$ in which $\beta \geq 1$ is an odd integer, is added to right hand side of 8. Therefore, for large value of $\gamma(t)$ the term $-\alpha\gamma^{\beta}(t)$ is large and convergence rate is much faster. Upper bound for $\gamma(t)$ to reach to zero for $\beta = 1$ is equal to*

$$t_0 + \frac{p}{\alpha(p-q)}\big(\ln(\alpha\gamma(t_0)^{1-\eta} + \mu) - \ln\mu\big) \tag{11}$$

According to the above lemmas, the sliding surface is defined as what proposed in [22]:

$$\mathbf{s} = \dot{\tilde{\mathbf{X}}} + \mathbf{\Gamma}_1\tilde{\mathbf{X}} + \mathbf{\Gamma}_2\tilde{\mathbf{X}}^p \tag{12}$$

in which $\tilde{\mathbf{X}} = \mathbf{X} - \mathbf{X}_d$ is difference between position and desired position of the robot, $\mathbf{\Gamma}_1, \mathbf{\Gamma}_2$ are positive definite diagonal constant matrices and $1/2 < p < 1$. The reason why p should be larger than 1/2 is as follows. Sliding surface proposed in Eq.(12) may be interpreted as a a velocity error term

$$\mathbf{s} = \dot{\mathbf{X}} - \dot{\mathbf{X}}_r \tag{13}$$

where $\dot{\mathbf{X}}_r = \dot{\mathbf{X}}_d - \mathbf{\Gamma}_1\tilde{\mathbf{X}} - \mathbf{\Gamma}_2\tilde{\mathbf{X}}^p$ and $\ddot{\mathbf{X}}_r = \ddot{\mathbf{X}}_d - \mathbf{\Gamma}_1\dot{\tilde{\mathbf{X}}} - p\mathbf{\Gamma}_2\tilde{\mathbf{X}}^{p-1}\dot{\tilde{\mathbf{X}}}$. Notice that $\ddot{\mathbf{X}}_r$ on the sliding surface $\mathbf{s} = 0$ is equal to

$$\begin{aligned}&\ddot{\mathbf{X}}_r = \ddot{\mathbf{X}}_d - \mathbf{\Gamma}_1\dot{\tilde{\mathbf{X}}} - p\mathbf{\Gamma}_2\text{diag}[\tilde{X}_1^{p-1}\tilde{X}_2^{p-1}\tilde{X}_3^{p-1}]\dot{\tilde{\mathbf{X}}} = \\ &\ddot{\mathbf{X}}_d + \mathbf{\Gamma}_1(\mathbf{\Gamma}_1\tilde{\mathbf{X}} + \mathbf{\Gamma}_2\tilde{\mathbf{X}}^p) + p\mathbf{\Gamma}_2\text{diag}[\tilde{X}_1^{p-1}\tilde{X}_2^{p-1}\tilde{X}_3^{p-1}] \\ &(\mathbf{\Gamma}_1\tilde{\mathbf{X}} + \mathbf{\Gamma}_2\tilde{\mathbf{X}}^p) = \ddot{\mathbf{X}}_d + \mathbf{\Gamma}_1^2\tilde{\mathbf{X}} + (1+p)\mathbf{\Gamma}_1\mathbf{\Gamma}_2\tilde{\mathbf{X}}^p + p\mathbf{\Gamma}_2\tilde{\mathbf{X}}^{2p-1}\end{aligned} \tag{14}$$

Therefore, p should be larger than 1/2 to ensure boundedness of $\ddot{\mathbf{X}}_r$.

Define the A-FTSM control law as follows

$$\begin{aligned}&\tau = -\mathbf{J}(\mathbf{X})^{\dagger}(\hat{\mathbf{M}}\ddot{\mathbf{X}}_r + \hat{\mathbf{G}} - \mathbf{K}_1\mathbf{s}^{\alpha_1} - \mathbf{K}_2\mathbf{s}^{\alpha_2}) = -\mathbf{J}(\mathbf{X})^{\dagger}\big(\mathbf{Y}(\ddot{\mathbf{X}}_r)\hat{\theta}_m \\ &- \mathbf{K}_1\mathbf{s}^{\alpha_1} - \mathbf{K}_2\mathbf{s}^{\alpha_2}\big)\end{aligned} \tag{15}$$

where $\mathbf{J}(\mathbf{X})^{\dagger} = \mathbf{J}(\mathbf{X})(\mathbf{J}(\mathbf{X})^T\mathbf{J}(\mathbf{X}))^{-1}$ is the right pseudo inverse of Jacobian matrix $\mathbf{J}(\mathbf{X})$, $\hat{\mathbf{M}}$ and $\hat{\mathbf{G}}$ are estimate of $\mathbf{M}$ and $\mathbf{G}$, respectively, $(\mathbf{K}_1, \mathbf{K}_2)$ are positive definite diagonal matrices, $\alpha_1 \geq 1$ is an odd integer and $0 < \alpha_2 < 1$ is ratio of two odd integers. The regressor form is equal to

$$\mathbf{Y}(\ddot{\mathbf{X}}_r)\hat{\theta}_m = \begin{bmatrix}\ddot{X}_{r_1} \\ \ddot{X}_{r_2} \\ \ddot{X}_{r_3}\end{bmatrix}\hat{m} \tag{16}$$

and adaption law is as follows

$$\dot{\hat{\theta}}_m = -\frac{\mathbf{s}^T\mathbf{Y}(\ddot{\mathbf{X}}_r)}{\gamma} \tag{17}$$

The block diagram of the proposed controller is shown in figure 3.

Theorem. *Consider the 3-DOF redundant cable driven robot with dynamics formulation 6, the control law 15 and the adaptation law 17. Then, $\tilde{\mathbf{X}}_r$ converge to zero in finite time.*

Proof. Substitute the control law 15 in dynamics formulation 6:

$$\begin{aligned}&\mathbf{M}(\mathbf{X})\ddot{\mathbf{X}} + \mathbf{C}(\mathbf{X}, \dot{\mathbf{X}})\dot{\mathbf{X}} + \mathbf{G}(\mathbf{X}) = -\mathbf{J}(\mathbf{X})^T\Big(- \mathbf{J}(\mathbf{X})^{\dagger}\big(\mathbf{Y}(\ddot{\mathbf{X}}_r)\hat{\theta}_m \\ &- \mathbf{K}_1\mathbf{s}^{\alpha_1} - \mathbf{K}_2\mathbf{s}^{\alpha_2}\big)\Big) = \mathbf{Y}(\ddot{\mathbf{X}}_r)\hat{\theta}_m - \mathbf{K}_1\mathbf{s}^{\alpha_1} - \mathbf{K}_2\mathbf{s}^{\alpha_2}\end{aligned} \tag{18}$$

Add $-\mathbf{Y}(\ddot{\mathbf{X}}_r)\theta_m = -\mathbf{M}\ddot{\mathbf{X}}_r - \mathbf{G}$ to both side of Eq. 18:

$$\mathbf{M}(\ddot{\mathbf{X}} - \ddot{\mathbf{X}}_r) = \mathbf{M}\dot{\mathbf{s}} = \mathbf{Y}(\ddot{\mathbf{X}}_r)\tilde{\theta}_m - \mathbf{K}_1\mathbf{s}^{\alpha_1} - \mathbf{K}_2\mathbf{s}^{\alpha_2} \tag{19}$$

in which $\tilde{\theta}_m = \hat{\theta}_m - \theta_m$.

Now consider the following Lyapunov function

$$V = \frac{1}{2}\mathbf{s}^T\mathbf{M}\mathbf{s} + \frac{1}{2}\gamma\tilde{\theta}^2 \tag{20}$$

Time derivative of 20 is as follows

$$\dot{V} = \mathbf{s}^T\mathbf{M}\dot{\mathbf{s}} + \gamma\tilde{\theta}_m\dot{\tilde{\theta}}_m \tag{21}$$

By replacing $\mathbf{M}\dot{\mathbf{s}}$ from 19 and noticing the fact that θ is a constant value, one may obtain the following equation

$$\begin{aligned}&\dot{V} = \mathbf{s}^T\big(\mathbf{Y}(\ddot{\mathbf{X}}_r)\tilde{\theta}_m - \mathbf{K}_1 s^{\alpha_1} - \mathbf{K}_2 s^{\alpha_2}\big) + \gamma\tilde{\theta}_m\dot{\hat{\theta}}_m = -\mathbf{K}_1 s^{\alpha_1+1} \\ &- \mathbf{K}_2 s^{\alpha_2+1} + \big(\mathbf{s}^T\mathbf{Y}(\ddot{\mathbf{X}}_r) + \gamma\dot{\hat{\theta}}_m\big)\tilde{\theta}_m\end{aligned} \tag{22}$$

By adaptation law 17, $\dot{V}$ is equal to

$$\dot{V} = -\mathbf{K}_1\mathbf{s}^{\alpha_1+1} - \mathbf{K}_2\mathbf{s}^{\alpha_2+1} \tag{23}$$

Considering Theorem 1 in [22], it can be shown that the sliding surface $\mathbf{s}$ converge to zero in finite time with the upper bound T according to lemma 1 as follows

$$T \leq t_0 + \frac{\max\big(\mathbf{s}^{1-\alpha_2}(t_0)\big)}{(1-\alpha_2)k_2^*} \tag{24}$$

in which $\boldsymbol{k}_2^*$ is the minimum element of $\mathbf{K}_2$.

On the sliding surface, the equation of motion of the robot reduces to

$$\dot{\tilde{\mathbf{X}}} + \mathbf{\Gamma}_1 \tilde{\mathbf{X}} + \mathbf{\Gamma}_2 \tilde{\mathbf{X}}^p = 0$$

Again consider lemma 1 and lemma 2. Upper bound for convergence time of $\mathbf{X}$ to $\mathbf{X}_d$ is

$$T' \leq T + \frac{\max\left(\tilde{\mathbf{X}}^{1-p}(T)\right)}{(1-p)\gamma_2^*} \tag{25}$$

in which γ_2^* is the minimum element of $\mathbf{\Gamma}_2$. □

Remark 1. *It is obvious from equations 24 and 25 that in order to reduce the convergence time, the gains $\mathbf{\Gamma}_2$ and $\mathbf{K}_2$ shall increase. Furthermore, as explained in lemma 2, by increasing $\mathbf{K}_1, \mathbf{\Gamma}_1$ the solution leads to faster convergence.*

Remark 2. *In contrast to previous works which select $\alpha_1 = 1$, we consider $\alpha_1 \geq 1$, because for larger value of* s*, the convergence time will be reduced.*

IV. Experimental Results

A. Description of the robot

ARAS–CAM robot is a four-actuator cable-driven robot with 3-DOF, which is shown in Fig. 1. In this robot, the end-effector is constrained by four cables connecting it to the anchor points on the base. The locations of these anchor points correspond to upper vertices of a hypothetical cube with dimensions $3.56m \times 7.05m \times 4.26m$. In fact, this cube represents the robot's workspace. The coordinates for these points along with the parameters of the robot are as follows.

$$\begin{bmatrix} x_{A_1} \\ y_{A_1} \\ z_{A_1} \end{bmatrix} = \begin{bmatrix} 3.56/2 \\ 7.05/2 \\ 4.26 \end{bmatrix} \quad \begin{bmatrix} x_{A_2} \\ y_{A_2} \\ z_{A_2} \end{bmatrix} = \begin{bmatrix} -3.56/2 \\ 7.05/2 \\ 4.26 \end{bmatrix}$$

$$\begin{bmatrix} x_{A_3} \\ y_{A_3} \\ z_{A_3} \end{bmatrix} = \begin{bmatrix} 3.56/2 \\ -7.05/2 \\ 4.26 \end{bmatrix} \quad \begin{bmatrix} x_{A_4} \\ y_{A_4} \\ z_{A_4} \end{bmatrix} = \begin{bmatrix} -3.56/2 \\ -7.05/2 \\ 4.26 \end{bmatrix}$$

$$m = 4.5Kg$$

Moreover, the actuators of ARAS-CAM are AC-servo motors directly coupled to the cables trough a drum mechanism. Capable of delivering a maximum of $24.4Kg.Cm$ of torque, this motors can create tension as high as $80N$ in the cables. As position sensor, a stereo camera modified to be strictly sensitive to IR light is used. For the purpose of position measurement, an infrared LED embedded on the end-effector is detected by the aforementioned vision system. After undergoing some geometrical transformations, coordinate systems of the vision system and the robot are co-registered.

Furthermore the gains of the controller are set as follows

$$\alpha_1 = 1 \qquad \alpha_2 = 7/9 \qquad p = 7/9$$

$$\mathbf{\Gamma}_1 = \begin{bmatrix} 6 & 0 \\ 0 & 6 \end{bmatrix} \qquad \mathbf{\Gamma}_2 = \begin{bmatrix} 1 & 0 \\ 0 & 1 \end{bmatrix}$$

$$\mathbf{K}_1 = \begin{bmatrix} 10 & 0 \\ 0 & 10 \end{bmatrix} \qquad \mathbf{K}_2 = \begin{bmatrix} 2 & 0 \\ 0 & 2 \end{bmatrix}$$

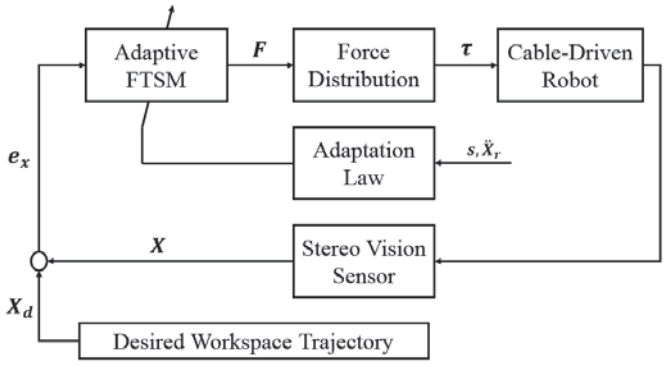

Fig. 3. Block diagram of the proposed adaptive FTSM controller.

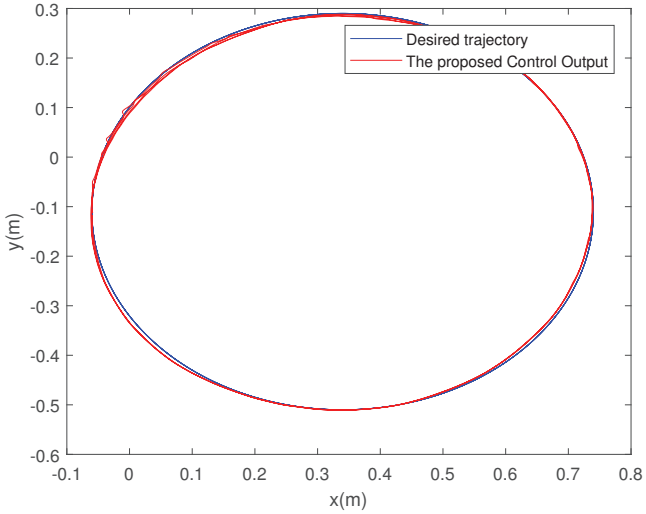

Fig. 4. Actual and desired position of the end-effector in the XY plane.

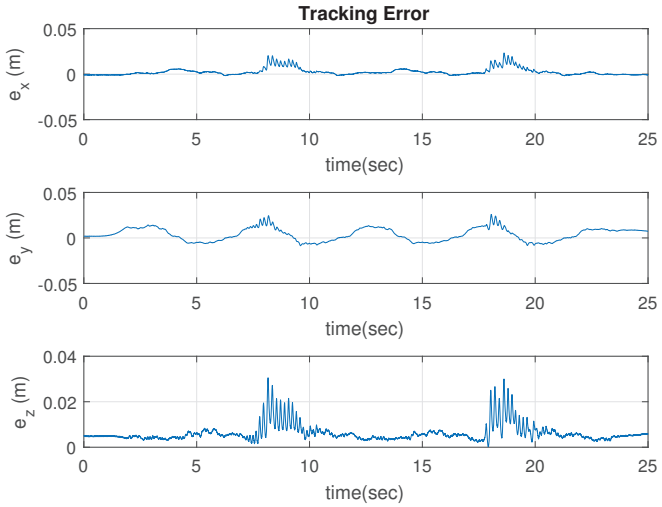

Fig. 5. Tracking error of the desired circular trajectory with a radius of 0.4 m.

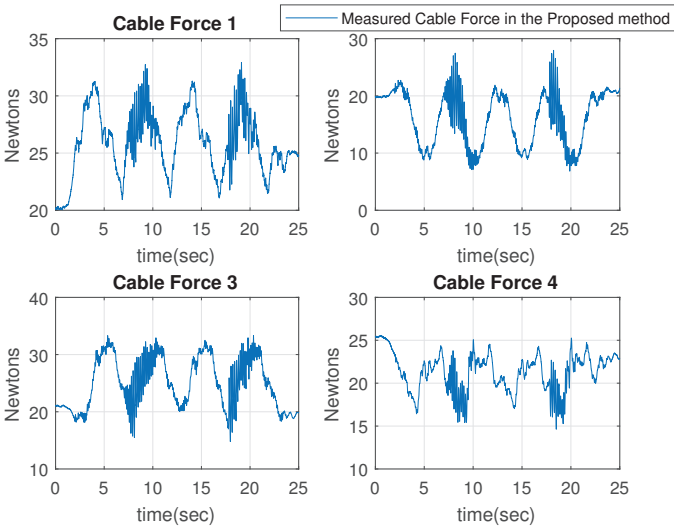

Fig. 6. Measured cable force during the execution of a circular trajectory.

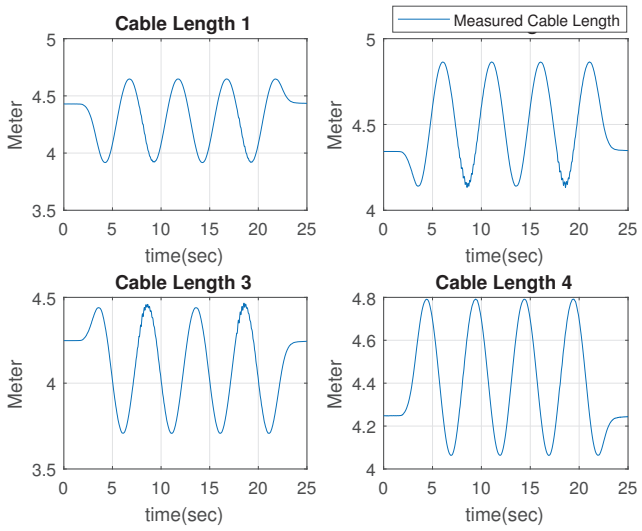

Fig. 7. Experimental results of cables length variation.

As previously noted, cable tension is of paramount importance in cable-driven parallel robots. For this reason, the reference trajectory is designed to maneuver the robot within feasible workspace [23] to ensure that the cable forces are positive.

B. Results

In order to demonstrate the effectiveness of the proposed adaptive FTSM controller, its performance on the ARAS-CAM cable-driven parallel robot is experimentally evaluated and the corresponding results are illustrated. This experiment has aimed to evaluate the performance of the proposed controller under dynamics uncertainties of the robot. It is assumed that the precise knowledge of the mass of the end-effector and the friction parameters of the actuators are not known in practice. For this purpose, a challenging circular trajectory with a radius of 0.4 m is considered in a constant height. Figure 4 shows the reference path on the XY plane that the robot follows with a suitable accuracy. Furthermore, figure 5 illustrates the tracking errors, which are less than two centimeters in worst case in all directions.

Figure 6 shows the cable's tension variations during the movement of the end-effector. As depicted in this figure none of cable forces are negative and all the cables are in tension. Therefore, the designed trajectory for the robot is within the feasible wrench workspace. Figure 7 shows the cable lengths within the robot's path. As shown in this figure, due to the circular path, length of all of the cables change sinusoidally as expected.

V. Conclusion and Future Work

Of paramount importance, trajectory tracking in the presence of uncertainties is the ultimate goal for all practical robotic applications. An FTSM-based adaptive controller for cable-driven parallel manipulators is proposed in this paper, in such a way to track the desired robot trajectory in the presence of dynamic uncertainties at different operating speed. In order to further improve the tracking capabilities of FTSM control, we have proposed to extend it with an adaptive control loop based on the dynamic model of the manipulator. The extended controller benefits from the advantages of both FTSM and adaptive control. In order to evaluate the effectiveness of the proposed controller, real-time experiments were conducted on ARAS-CAM, a cable-driven suspended parallel robot. The obtained results have shown that tracking performance of the proposed controller is very suitable in practice. Our future work focuses on the design of a robust adaptive FTSM in presence of kinematic and Jacobian uncertainties as well as unmodeled dynamics.

References

[1] C. Gosselin, "Cable-driven parallel mechanisms: state of the art and perspectives," *Mechanical Engineering Reviews*, vol. 1, no. 1, pp. DSM0004–DSM0004, 2014.

[2] Y. Patel and P. George, "Parallel manipulators applications—a survey," *Modern Mechanical Engineering*, vol. 2, no. 03, p. 57, 2012.

[3] X. Tang, "An overview of the development for cable-driven parallel manipulator," *Advances in Mechanical Engineering*, vol. 6, p. 823028, 2014.

[4] J. Lenarcic and M. Stanišić, *Advances in Robot Kinematics: Motion in Man and Machine*. Springer, 2010.

[5] D. Zanotto, G. Rosati, S. Minto, and A. Rossi, "Sophia-3: A semiadaptive cable-driven rehabilitation device with a tilting working plane," *IEEE Transactions on Robotics*, vol. 30, no. 4, pp. 974–979, 2014.

[6] X. Duan, Y. Qiu, Q. Duan, and J. Du, "Calibration and motion control of a cable-driven parallel manipulator based triple-level spatial positioner," *Advances in Mechanical Engineering*, vol. 6, p. 368018, 2014.

[7] R. Verhoeven, M. Hiller, and S. Tadokoro, "Workspace, stiffness, singularities and classification of tendon-driven stewart platforms," in *Advances in robot kinematics: Analysis and Control*, pp. 105–114, Springer, 1998.

[8] R. Bostelman, J. Albus, N. Dagalakis, A. Jacoff, and J. Gross, "Applications of the nist robocrane," in *Proceedings of the 5th International Symposium on Robotics and Manufacturing*, pp. 14–18, 1994.

[9] S. Qian, B. Zi, and H. Ding, "Dynamics and trajectory tracking control of cooperative multiple mobile cranes," *Nonlinear Dynamics*, vol. 83, no. 1-2, pp. 89–108, 2016.

[10] H. R. Fahham, M. Farid, and M. Khooran, "Time optimal trajectory tracking of redundant planar cable-suspended robots considering both tension and velocity constraints," *Journal of Dynamic Systems, Measurement, and Control*, vol. 133, no. 1, p. 011004, 2011.

[11] R. Babaghasabha, M. A. Khosravi, and H. D. Taghirad, "Adaptive control of kntu planar cable-driven parallel robot with uncertainties in dynamic and kinematic parameters," in *Cable-Driven Parallel Robots*, pp. 145–159, Springer, 2015.

[12] S. Khalilpour, R. Khorrambakht, M. Harandi, H. Taghirad, and P. Cardou, "Robust dynamic sliding mode control of a deployable cable driven robot," in *Electrical Engineering (ICEE), Iranian Conference on*, pp. 863–868, IEEE, 2018.

[13] T.-H. S. Li and Y.-C. Huang, "Mimo adaptive fuzzy terminal sliding-mode controller for robotic manipulators," *Information Sciences*, vol. 180, no. 23, pp. 4641–4660, 2010.

[14] C.-F. Hsu and B.-K. Lee, "Fpga-based adaptive pid control of a dc motor driver via sliding-mode approach," *Expert Systems with Applications*, vol. 38, no. 9, pp. 11866–11872, 2011.

[15] K. Saoudi and M. Harmas, "Enhanced design of an indirect adaptive fuzzy sliding mode power system stabilizer for multi-machine power systems," *International Journal of Electrical Power & Energy Systems*, vol. 54, pp. 425–431, 2014.

[16] S. Ding, S. Li, and W. X. Zheng, "Brief paper: new approach to second-order sliding mode control design," *IET Control Theory & Applications*, vol. 7, no. 18, pp. 2188–2196, 2013.

[17] S. Mobayen, V. J. Majd, and M. Sojoodi, "An lmi-based composite nonlinear feedback terminal sliding-mode controller design for disturbed mimo systems," *Mathematics and Computers in Simulation*, vol. 85, pp. 1–10, 2012.

[18] Y. Wu, B. Wang, and G. Zong, "Finite-time tracking controller design for nonholonomic systems with extended chained form," *IEEE Transactions on Circuits and Systems II: Express Briefs*, vol. 52, no. 11, pp. 798–802, 2005.

[19] X. Yu and M. Zhihong, "Fast terminal sliding-mode control design for nonlinear dynamical systems," *IEEE Transactions on Circuits and Systems I: Fundamental Theory and Applications*, vol. 49, no. 2, pp. 261–264, 2002.

[20] H. D. Taghirad, *Parallel robots: mechanics and control*. CRC press, 2013.

[21] E. Moulay and W. Perruquetti, "Finite time stability and stabilization of a class of continuous systems," *Journal of Mathematical analysis and applications*, vol. 323, no. 2, pp. 1430–1443, 2006.

[22] S. Yu, G. Guo, Z. Ma, and J. Du, "Global fast terminal sliding mode control for robotic manipulators," *International Journal of Modelling, Identification and Control*, vol. 1, no. 1, pp. 72–79, 2006.

[23] M. Gouttefarde, J.-P. Merlet, and D. Daney, "Wrench-feasible workspace of parallel cable-driven mechanisms," in *Robotics and Automation, 2007 IEEE International Conference on*, pp. 1492–1497, IEEE, 2007.